arXiv:1702.04331v1 [cond-mat.supr-con] 14 Feb 2017

Low Energy Phonons in $Bi_2Sr_2CaCu_2O_{8+\delta}$ and their Possible Interaction with Electrons Measured by Inelastic Neutron Scattering

A. M. Merritt[1], J.-P. Castellan[2], S. R. Park[3], J. A. Fernandez-Baca[4,5], G. D. Gu[6], D. Reznik[1]*

1. *Department of Physics, University of Colorado - Boulder, Boulder, Colorado 80305, USA*
2. *Karlsruhe Institute of Technology, Karlsruhe, Germany*
3. *Incheon National University, Incheon, Korea*
4. *Quantum Condensed Matter Division, Oak Ridge National Laboratory, Oak Ridge, Tennessee 37831, USA*
5. *Department of Physics and Astronomy, University of Tennessee, Knoxville, Tennessee 37996, USA*
6. *Condensed Matter Physics & Materials Science Department, Brookhaven National Laboratory, Upton, New York 11973, USA*

* *Corresponding author: Dmitry.Reznik@colorado.edu*

Angle-resolved photoemission (ARPES) experiments on copper oxide superconductors revealed enigmatic kinks in electronic dispersions near 10 meV presumably due to phonons or impuritites. We used inelastic neutron scattering to measure phonon branches below 15 meV in a large single crystal sample of optimally-doped $Bi_2Sr_2CaCu_2O_{8+\delta}$ (BSCCO). The high quality dataset covered several Brilloiun zones with different final energies. In addition to acoustic branches, optic branches disperse from 4 meV and 7 meV zone center energies. The 4 meV branch interacts with acoustic phonons at small wavevectors, which destroys the LA character of the acoustic branch beyond 0.15 reciprocal lattice units. We propose a mechanism that explains the low energy electronic dispersion features based on this observation.

The role of electron-phonon coupling in copper oxide superconductors is still not understood. Early experiments and calculations indicated that it was not important, [1, 2], but later work suggested it is very strong for select phonons [3–8].

Angle-resolved photoemission (ARPES) revealed pronounced kinks in the electronic dispersions, often interpreted in terms of interactions of electronic quasiparticles with Bosonic modes [9, 10]. Most previous work focused on the analysis of the ARPES features between 30 and 80 meV, but more recently a kink near 10 meV has been discovered [11–14]. In the majority of cases, optic phonons are natural candidates, although a number of mutually-exclusive explanations for the 10 meV kink have been proposed [11, 15, 16]. The most unusual property of this kink is an apparent absence of gap-referencing, where the kink should appear at $\omega_{\rm ph} + \Delta_{\rm max} > 30\,$meV (Maximum superconducting gap $\Delta_{\rm max} \sim 30\,$meV) [13]. This gap-referencing is expected from a flat Bosonic mode with a wavevector $\mathbf{q}$-independent mode-phonon coupling matrix element.

Here we report results of comprehensive neutron scattering measurements of low energy phonon dispersions in BSCCO in the energy range relevant for the ARPES kink. We show that the interaction of the longitudinal acoustic (LA) branch with the lowest optic branch around 4 meV (Fig. 1a) limits electronic scattering by the acoustic phonon to small wavevectors. As a result, the phonon can only scatter electrons with small crystal momentum transfer in the ab-plane. This forward scattering places nodal electron on nearby sections of the Fermi surface where the superconducting gap is small (Fig. 1b). Therefore, the kink at the node appears below the maximum of the superconducting gap via the mechanism similar to the one proposed by Johnston et al. [15].

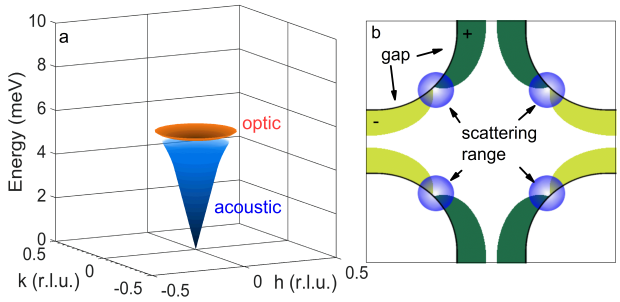

FIG. 1. Schematic of low-energy phonon dispersions relevant for the ARPES kink and forward scattering near the Fermi surface. (a) The blue cone/orange disc indicates acoustic/lowest optic phonon dispersion at small wavevectors consistent with our measurements. (b) Schematic of the Fermi surface, superconducting gap and coupling in BSCCO. The black lines denotes the Fermi surface. Yellow and green indicate gaps (of opposite signs with minima at the nodes). The semitransparent blue circles represent where nodal electrons are scattered by the LA phonon provided kinematic constraints are met. The variation in transparency of the blue circles represents the intensity of the scattering that is proportional to $|\mathbf{q}|$.

Measurements were performed on the 1T triple-axis spectrometer at the Orphée reactor (Laboratoire Léon Brillouin, France) using PG002 monochromator/analyzer in the standard open collimation configuration and in a similar condition on the HB-3 spectrometer at the High Flux Isotope Reactor (HFIR) at Oak Ridge National Laboratory. The sample was a large single crystal grown with the floating-zone technique as detailed in Ref. [17]. The sample was mounted in a closed-cycle refrigerator.

We looked at every experimentally accessible Brillouin zone around **Q**=(0,0,L) as well as 200 and 202 using fixed final energies E_f=8, 13.2, and 14.7 meV. For the majority of the measurements the sample was mounted in the H0L scattering plane. We measured phonon dispersions along the a* and c*-directions in reciprocal space with some data also obtained along the HH0 and H-H0 directions. The energy region around 10 meV in the data measured with E_f=8 meV is not used, because it corresponds to a $2k_f = 3k_i$ condition.

In tetragonal structures the LA branch always forms a cone near the zone center in the h-k plane (in our notation h is along a*, k is along b* and l is along c*) as shown in Fig. 1a. Thus it is sufficient to measure its dispersion along the h-direction to know the entire dispersion at small **q**. According to standard theory, the LA branch should couple to electrons because it modulates the density of the material [18]. In simple materials the LA branch extends all the way to the zone boundary. However in perovskite oxides the LA branch interacts with low-energy optic branches [19, 20], which radically alters its eigenvector.

We carefully tracked the character of the acoustic branches by comparing intensities in several Brillouin zones. Acoustic phonon intensity is proportional to the intensities of the adjacent Bragg peaks, i.e. the data in several zones allows us to identify the phonon with the LA eigenvector by this property. For longitudinal phonons dispersing in the ab plane we performed measurements in the Brillouin zone adjacent to the strong Bragg peak at **Q**=(2,0,0) and in the zone adjacent to a weak Bragg peak at **Q**=(2,0,2).

Figure 2d,e shows that strong optic phonons disperse from the zone center energies at **Q**=(2,0,0) and **Q**=(2,0,2) at 4 meV and 7 meV (also see supplementary material Fig. S1). The (2,0,0) Bragg peak is very strong, which maximizes the intensity of acoustic phonons in the adjacent zone. On the other hand, the (2,0,2) Bragg peak is much weaker, which makes the acoustic phonons too weak to be observed and the optic one stronger. The appearance of the 4 meV phonon near **Q**=(2,0,2) vs. **Q**=(2,0,0) indicates that this phonon originates primarily from the out-of-phase in-plane vibrations of Bi. The acoustic phonon disperses up to 4 meV at h=0.15 where it starts to deviate from the linear dispersion expected for acoustic phonons at small **q**. The signal weakens and becomes very broad at higher h.

This difference between the zone adjacent to **Q**=(2,0,0) and the zone adjacent to **Q**=(2,0,2) is only seen up to h=0.15 where the acoustic branch becomes broader, and its energy deviates from the linear dispersion(Figs. 2i, 3). In addition, the acoustic phonon intensity drops from h=0.1 to 0.15, (Fig. 3c,d) which indicates that eigenvector is no longer of purely LA character. At **q**=(0.2,0,0) the phonons have the same intensity in the two zones, i.e. at this q there is no phonon that is predominantly LA.

At this wavevector the low-lying optic branch becomes very broad in energy with phonon tails extending down to 2.5 meV. Aside from the Bose factor, this behavior appears to be the same at low and room temperature (Fig. 3), although interpretation of the data is harder at low temperature due to the small intensities. The region between h=0.2 and 0.35 is characterized by broad line shapes followed by the recovery of a narrower lineshape at h=0.35 and 0.4. A similar effect has been observed at the same wavevectors in a few other branches in all previously investigated copper oxide superconductors [7] [21], but not in the lowest-energy longitudinal branch. We carefully checked if the phonon broadening persists down to lower energies by performing h-scans at 1.5 meV, but found no evidence for a low-energy tail around h=0.25-0.3 (see supplementary material Fig. S3). Based on results presented in Ref. [22], it is probably related to the structural supermodulation. We plan to investigate this feature in more detail in the future, which should elucidate its origin.

We observed other optic phonon branches as well. The nearly flat branch originating from 6.5 meV is primarily c-axis polarized as it has a much stronger intensity when L is large, i.e. when **Q** is parallel to the c-axis (Fig. 2i). There are only two zones in which c-axis-polarized phonons are clearly observable. Acoustic/optic phonons are strong at **Q**=(H,0,12) / **Q**=(H,0,14) respectively. The 6.5 meV feature at **Q**=(0,0,14) is broader than the instrument resolution and most probably, two separate modes are observed (Fig. 2a,b). One of these, at 7 meV, has some in-plane polarized atomic displacements since it is also seen at in-plane wave vectors (Fig. 2g,h). The optic mode disperses upwards, and merges with the acoustic mode near h=0.3. At this point the branches mix and lose their pure acoustic/optic character. Only one branch is seen past this point. The other one acquires and eigenvector whose structure factor makes it weak in this zone.

Phonon dispersions in the L-direction are nearly flat due to the quasi-2D character of BSCCO (Fig. 2c,f). The LA mode stays at low energies with the zone boundary energy of 2.5 meV. The TA mode has a similar dispersion and optic modes are nearly flat (Fig. 2f). Momentum-energy cuts in different Brillouin zones are shown in Fig. S4 of the supplementary material. Additional scans along the longitudinal and transverse directions near the (2,2,0) Bragg peak are reported in Fig. S2 of the supplementary material. They are consistent with Figs. 1 and 2.

The data shown in Figs. 2, 3 allow us to understand the ARPES kink feature at 10meV employing the minimum of assumptions. Longitudinal acoustic phonons couple to electrons because they modulate the density of the material [18]. However, once they interact with the optic phonon away from the zone center, their eigenvector changes. Since electron-phonon matrix elements sensitively depends on the phonon eigenvectors, we ex-

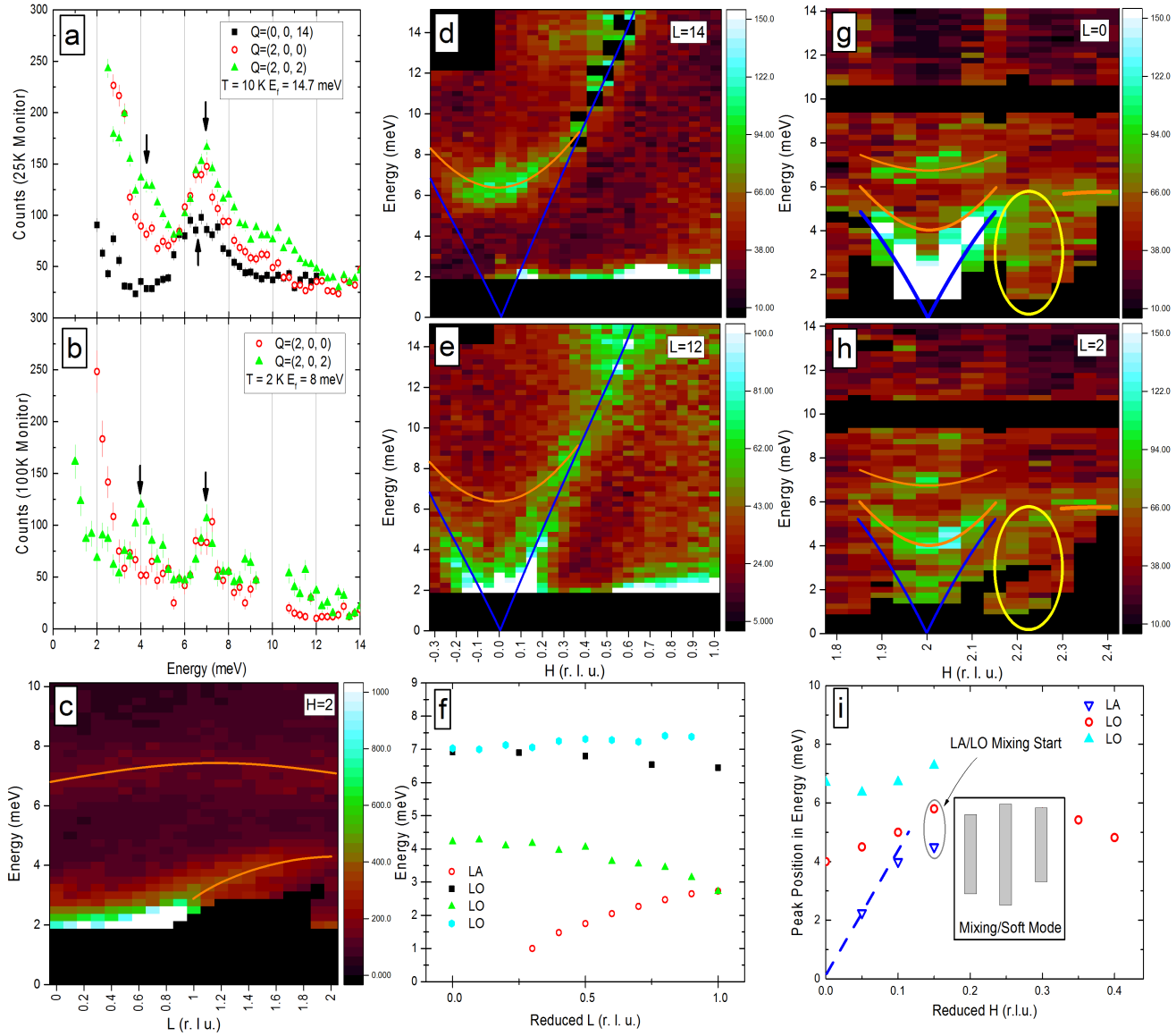

FIG. 2. Main experimental results at low temperature. (a, b) Energy scans at zone center. Arrows denote phonon peaks at 4, 6.5, and 7 meV. (c-e, g, h) Momentum-energy cuts. Solid lines denote phonon dispersions: blue for acoustic and orange for optic. Yellow oval represents the interaction/soft mode region (see text). Final neutron energy for (a, c, d, e) was E_f=14.7 meV. Final neutron energy for (b, g, h) was E_f=8 meV. (f) Peak positions for phonons dispersing along L. (i) Peak positions for phonons dispersing along H. Dashed line indicates a linear dispersion expected of the LA branch (blue triangles) in the absence of interaction with the LO branch (red circles).

pect electron-phonon coupling to become suppressed as the mode loses its LA character beyond h=0.15 and the standard theory would no longer apply. It is possible that phonons of different character couple to electrons as well. However, in the case of cuprates, density functional theory shows that such coupling should be weak. Previous experiments found strong electron-optic phonon coupling only in the Cu-O bond stretching branch around 70meV and the buckling branch that starts at the B_{1g} mode near 40meV, which can be considered as exceptional. No signs of strong electron-phonon interaction in BSCCO optic phonons have been reported otherwise despite numerous Raman and IR investigations [23–28].

Thus only forward scattering of electrons by LA phonons in the ab-plane is allowed and electrons can scatter only into the nearby regions of the Fermi surface as shown for the nodal electrons in Fig. 1b. The gap there cannot be much bigger than the gap where the electron originates, hence the kink appears below T_c offset by a fixed energy from the superconducting gap going

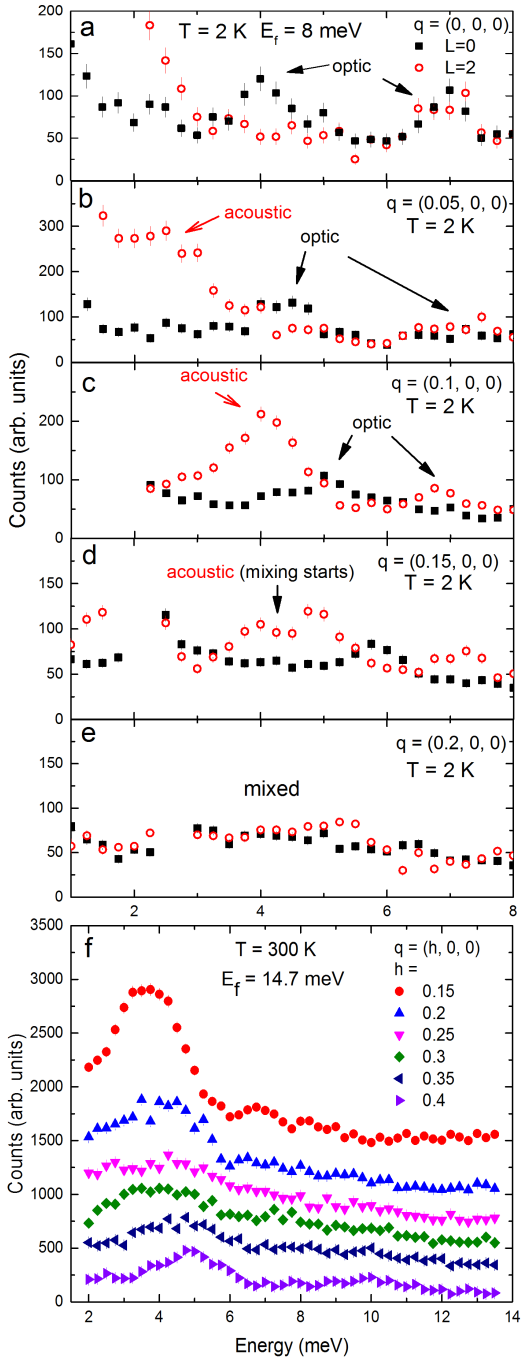

FIG. 3. Longitudinal phonons along the h-direction. (a-e) T=2K, E_f=8meV. Black squares: Total wavevector **Q** is (2,0,0)+**q**. Black squares are for L=0, open Red circles: Total wavevector **Q** is (2,0,2)+**q**. (f) T=300K, E_f=14.7meV. Total wavevector **Q** is (2,0,0)+**q**

.

around the Fermi surface. This offset energy should be much smaller than the maximum of the superconducting gap. Ref. [15] proposed a similar falloff in the electron coupling strength via a different mechanism and showed that this falloff is all that is required to reproduce the ARPES data. Their calculation of the ARPES features should still apply regardless of the exact mechanism of suppression of the electron-phonon matrix element.

Rameau et al. [11] proposed that the 10 meV kink was caused by one of the A_{1g} Raman modes [26, 27] with c-axis polarization. We see these modes near 6.5 meV in the neutron data. Fig. 2 shows that the c-axis optic phonon has a nearly flat dispersion up to **q**=(0.2,0,0). A similar dispersion is expected along the (h,h,0)-direction. Such a phonon will scatter electrons at least half way to the node where the gap is around 15 meV. This scattering will produce the kink in the superconducting state at 15+7=22 meV, which does not agree with experiment. Some theoretical models predict that the coupling is concentrated within 0.15 r.l.u. of the zone center [29, 30]. In this case, the nodal kink would be smeared inside the region between 7 and 12 meV. In experiments it appears to be sharper than that. Furthermore there is no evidence from Raman and IR that this phonon couples to electrons near the Fermi surface, such as softening below T_c [23–28].

To conclude, we observed the interaction of the low-lying optic branch with the longitudinal acoustic branch at small wavevectors and showed how it leads the low-energy electronic dispersion kinks.

A.M. and D.R. were supported by the DOE, Office of Basic Energy Sciences, Office of Science, under Contract No. de-sc0006939. G. G. was supported by the Office of Basic Energy Sciences (BES), Division of Materials Sciences and Engineering, U.S. Department of Energy (DOE), under Contract No. de-sc0112704. A portion of this research used resources at the High Flux Isotope Reactor, a DOE Office of Science User Facility operated by the Oak Ridge National Laboratory.

[1] B. Batlogg, R. J. Cava, A. Jayaraman, R. B. van Dover, G. A. Kourouklis, S. Sunshine, D. W. Murphy, L. W. Rupp, H. S. Chen, A. White, K. T. Short, A. M. Mujsce, and E. A. Rietman, Phys. Rev. Lett. **58**, 2333 (1987).
[2] C. Thomsen, H. Mattausch, M. Bauer, W. Bauhofer, R. Liu, L. Genzel, and M. Cardona, Solid State Communications **67**, 1069 (1988).
[3] J. P. Franck, J. Jung, M. A. K. Mohamed, S. Gygax, and G. I. Sproule, Physica B: Condensed Matter **169**, 697 (1991).
[4] C. Thomsen, Advanced Materials **4**, 341 (1992).
[5] Z.-X. Shen, A. Lanzara, S. Ishihara, and N. Nagaosa, Philosophical Magazine Part B **82**, 1349 (2002).
[6] C. Gadermaier, A. S. Alexandrov, V. V. Kabanov, P. Kusar, T. Mertelj, X. Yao, C. Manzoni, D. Brida, G. Cerullo, and D. Mihailovic, Phys. Rev. Lett. **105**, 257001 (2010).
[7] D. Reznik, Advances in Condensed Matter Physics **2010**, e523549 (2010).
[8] D. Reznik, Physica C: Superconductivity Stripes and Electronic Liquid Crystals in Strongly Correlated Ma-

terials, **481**, 75 (2012).
[9] T. Cuk, F. Baumberger, D. H. Lu, N. Ingle, X. J. Zhou, H. Eisaki, N. Kaneko, Z. Hussain, T. P. Devereaux, N. Nagaosa, and Z.-X. Shen, Phys. Rev. Lett. **93**, 117003 (2004).
[10] D. Reznik, G. Sangiovanni, O. Gunnarsson, and T. P. Devereaux, Nature **455**, E6 (2008).
[11] J. D. Rameau, H.-B. Yang, G. D. Gu, and P. D. Johnson, Phys. Rev. B **80**, 184513 (2009).
[12] H. Anzai, A. Ino, T. Kamo, T. Fujita, M. Arita, H. Namatame, M. Taniguchi, A. Fujimori, Z.-X. Shen, M. Ishikado, and S. Uchida, Phys. Rev. Lett. **105**, 227002 (2010).
[13] N. C. Plumb, T. J. Reber, J. D. Koralek, Z. Sun, J. F. Douglas, Y. Aiura, K. Oka, H. Eisaki, and D. S. Dessau, Phys. Rev. Lett. **105**, 046402 (2010).
[14] I. M. Vishik, W. S. Lee, F. Schmitt, B. Moritz, T. Sasagawa, S. Uchida, K. Fujita, S. Ishida, C. Zhang, T. P. Devereaux, and Z. X. Shen, Phys. Rev. Lett. **104**, 207002 (2010).
[15] S. Johnston, I. M. Vishik, W. S. Lee, F. Schmitt, S. Uchida, K. Fujita, S. Ishida, N. Nagaosa, Z. X. Shen, and T. P. Devereaux, Phys. Rev. Lett. **108**, 166404 (2012).
[16] S. H. Hong, J. M. Bok, W. Zhang, J. He, X. J. Zhou, C. M. Varma, and H.-Y. Choi, Phys. Rev. Lett. **113**, 057001 (2014).
[17] J. S. Wen, Z. J. Xu, G. Y. Xu, M. Hücker, J. M. Tranquada, and G. D. Gu, Journal of Crystal Growth **310**, 1401 (2008).
[18] G. Mahan, *Many-Particle Physics — Gerald D. Mahan — Springer* (2000).
[19] L. Pintschovius, D. Reznik, W. Reichardt, Y. Endoh, H. Hiraka, J. M. Tranquada, H. Uchiyama, T. Masui, and S. Tajima, Physical Review B **69** (2004), 10.1103/PhysRevB.69.214506.
[20] L. Pintschovius, phys. stat. sol. (b) **242**, 30 (2005).
[21] M. Le Tacon, A. Bosak, S. M. Souliou, G. Dellea, T. Loew, R. Heid, K.-P. Bohnen, G. Ghiringhelli, M. Krisch, and B. Keimer, Nat Phys **10**, 52 (2014).
[22] C. J. Bonnoit, D. R. Gardner, R. Chisnell, A. H. Said, Y. Okada, T. Kondo, T. Takeuchi, H. Ikuta, D. E. Moncton, and Y. S. Lee, (2012), arXiv:1202.4994.
[23] M. Kakihana, M. Osada, M. Käll, L. Börjesson, H. Mazaki, H. Yasuoka, M. Yashima, and M. Yoshimura, Phys. Rev. B **53**, 11796 (1996).
[24] N. N. Kovaleva, A. V. Boris, T. Holden, C. Ulrich, B. Liang, C. T. Lin, B. Keimer, C. Bernhard, J. L. Tallon, D. Munzar, and A. M. Stoneham, Phys. Rev. B **69**, 054511 (2004).
[25] A. A. Tsvetkov, D. Dulić, D. van der Marel, A. Damascelli, G. A. Kaljushnaia, J. I. Gorina, N. N. Senturina, N. N. Kolesnikov, Z. F. Ren, J. H. Wang, A. A. Menovsky, and T. T. M. Palstra, Phys. Rev. B **60**, 13196 (1999).
[26] R. Liu, M. V. Klein, P. D. Han, and D. A. Payne, Phys. Rev. B **45**, 7392 (1992).
[27] S. Martinez, A. Zwick, M. A. Renucci, H. Noel, and M. Potel, Physica C: Superconductivity **200**, 307 (1992).
[28] O. V. Misochko and E. Y. Sherman, J. Phys.: Condens. Matter **12**, 9095 (2000).
[29] M. L. Kulić and R. Zeyher, Phys. Rev. B **49**, 4395 (1994).
[30] R. Zeyher and M. L. Kulić, Phys. Rev. B **53**, 2850 (1996).